Fish and Shellfish Immunology 93 (2019) 851–862

Contents lists available at ScienceDirect

Fish and Shellfish Immunology

journal homepage: www.elsevier.com/locate/fsi

Full length article

Comparative proteomic investigation of *Marsupenaeus japonicus* hepatopancreas challenged with *Vibrio parahaemolyticus* and white spot syndrome virus

Xianyun Ren[a,b], Yunbin Zhang[a,b,c], Ping Liu[a,b], Jian Li[a,b,*]

[a] Key Laboratory for Sustainable Utilization of Marine Fisheries Resources, Ministry of Agriculture, Yellow Sea Fisheries Research Institute, Chinese Academy of Fishery Sciences, Qingdao, PR China
[b] Function Laboratory for Marine Fisheries Science and Food Production Processes, Qingdao National Laboratory for Marine Science and Technology, Qingdao, PR China
[c] College of Fisheries and Life Science, Shanghai Ocean University, Shanghai, China

ARTICLE INFO

Keywords:
WSSV
Vibrio parahaemolyticus
IBT
Marsupenaeus japonicas
Phagocytosis
Apoptosis

ABSTRACT

This study aimed to use isobaric tags (IBTs) to investigate the immune response of the hepatopancreas of *Marsupenaeus japonicas* infected with *Vibrio parahaemolyticus* or white spot syndrome virus (WSSV). Liquid chromatography-tandem mass spectrometry and protein sequencing identified 1005 proteins. Among them, 109 proteins were upregulated and 94 were downregulated after *V. parahaemolyticus* infection. After WSSV infection, 130 proteins were identified as differentially abundant, including 88 that were upregulated and 42 were downregulated. Fifty-four proteins were identified as differentially abundant after both *V. parahaemolyticus* and WSSV infection. A number of proteins related to cytoskeletal processes, including actin and myosin, and apoptosis-related proteins were upregulated in shrimp after *V. parahaemolyticus* and WSSV infection, indicating that phagocytosis and apoptosis may be involved in the response to in *V. parahaemolyticus* or WSSV infection. Quantitative real-time PCR was carried out to verify the reliability of the proteomic data. These data provide a basis to characterize the immunity-related processes of shrimp in response to infection with WSSV or *V. parahaemolyticus*.

1. Introduction

Marsupenaeus japonicus (kuruma shrimp) is a valuable marine aquaculture crustacean species in the Indo-West Pacific region [1]. Its economic value led to China producing more than 52,466 tons of the shrimp in 2017 [2]. Although *M. japonicus* is one of the three main farmed shrimp species worldwide, its economic exploitation has been hindered by outbreaks of serious bacterial and viral diseases [3,4]. White spot syndrome virus (WSSV) and acute hepatopancreatic necrosis disease (AHPND) are the major shrimp pathogens, which together can cause devastating mortality and large economic losses [5,6].

To develop strategies to prevent and treat these diseases, more detailed knowledge about the shrimp immune system and its immune responses to invading pathogens are required. To determine the molecular mechanisms responsible for the immune response to WSSV, proteomic studies have been conducted for the Chinese shrimp *Fenneropenaeus chinensis* [7], the white shrimp *Litopenaeus vannamei* [8], and the mud crab *Scylla paramamosain* [9]. However, no such study has been conducted for the infection of shrimp by *Vibrio parahaemolyticus*.

Determining shrimp's response to different types of pathogen, particularly the similarities and differences in the molecular responses of the shrimp immune system under challenge by different pathogens, will help to construct control strategies for the prevention of these infections. However, as far as we know, no study has reported a comparison of the protein expression patterns of shrimp challenged by *V.*

Abbreviations: IBT, isobaric tag; iTRAQ, isobaric tags for relative and absolute quantitation; WSSV, white spot syndrome virus; AHPND, acute hepatopancreatic necrosis disease; AMPs, antimicrobial peptides; DTT, dithiothreitol; KEGG, Kyoto Encyclopedia of Genes and Genomes; LC-MS/MS, liquid chromatography-tandem mass spectrometry; RT-PCR, real-time polymerase chain reaction; GO, gene ontology; MAPK, mitogen-activated protein kinase; CAMs, cell adhesion molecules; DAPs, differentially abundant proteins; GST, glutathione-S-transferase; α_2M, α_2-macroglobulin; PBS, phosphate-buffered saline; proPO, prophenoloxidase; PAP, phagocytosis activating protein; PRPs, pattern recognition proteins; SR-B, scavenge receptor B; TLR, toll-like receptor; BGs, β-1,3-glucans; LPS, lipopolysaccharides; PG, peptidoglycan; HSP, heat shock protein

* Corresponding author.Yellow Sea Fisheries Research Institute, Chinese Academy of Fishery Sciences, 106 Nanjing Road, Qingdao, 266003, PR China.
E-mail address: lijian@ysfri.ac.cn (J. Li).

https://doi.org/10.1016/j.fsi.2019.08.039
Received 24 March 2019; Received in revised form 10 August 2019; Accepted 14 August 2019
Available online 17 August 2019
1050-4648/

parahaemolyticus and WSSV. In the present study, liquid chromatography-tandem mass spectrometry (LC-MS/MS) combined with 10-plex IBT technology were used to determine the differences in protein levels in shrimp challenged by *V. parahaemolyticus* and WSSV. The result may increase our understanding of shrimp shrimp-virus interactions and antiviral immunity.

2. Materials and methods

2.1. Pathogen challenge

M. japonicus were infected with *V. parahaemolyticus* and WSSV as described in our previous study [11]. The shrimps were randomly divided three groups (n = 9): The *V. parahaemolyticus*-infected group, the group infected with WSSV-infected group, and the negative control group. For the *V. parahaemolyticus*-infected group, each shrimp was intramuscularly injected with 100 μL of filtered supernatant obtained from *M. japonicus* suffering from AHPND at a cell density of 10^6 colony-forming units (cfu)/mL. Similarly, animals in the WSSV-infected group were injected with 100 μL of filtered supernatant obtained from WSSV-infected *M. japonicus* (10^7 copies/mL). Infection was confirmed using PCR, as described previously [10]. The control group received 100 μL of phosphate-buffered saline (PBS, pH 7.4) per individual. Ten individuals from each group were randomly selected at 24 h post-infection, and hepatopancreas tissue was dissected and preserved in liquid nitrogen until protein extraction. Three biological replicates were performed in the three experimental groups, providing a total of nine samples.

2.2. Isobaric-tagged isotope dilution LC − MS/MS

Proteins were isolated from shrimp hepatopancreas and dissolved in lysis buffer or triethylammonium bicarbonate containing 2 mM ethylenediaminetetraacetic acid and 1 mM phenylmethylsulfonyl fluoride. The peptides were then analyzed using isobaric-tagged isotope dilution LC − MS/MS as described previously [12].

2.3. Data analysis

The TripleTOF 5600 System (SCIEX, Framingham, MA, USA), a hybrid triple quadrupole time-of-flight mass spectrometer, was used to acquire the data, and was operated as described previously [12].

2.4. Quantification and identification of proteins

The raw data from.LC-MS/MS were converted into MGF files and the proteins were identified as described previously [13]. Quantification analysis was performed using the IBT-based method [12]. Based on *t* tests, a *p*-value less than 0.05 and a fold change more than 1.20 or less than 0.83 were used as thresholds to screen for differentially abundant proteins (DAPs).

2.5. Gene ontology (GO) and kyoto encyclopedia for genes and genomes (KEGG) pathway enrichment analyses

Go and KEGG pathway enrichment analysis was performed as described previously [12]. In the analysis of enriched GO pathways and terms associated with the DAPs, $p < 0.05$ was considered statistically significant.

2.6. Verification of differentially abundant proteins

The genes corresponding to selected upregulated proteins in infected shrimps and the primers to detect these genes are listed in Supplemental Table 1. Gene expression was analyzed using RT-PCR as described previously [13]. The PCR protocol included initial denaturation at 95 °C for 10 min, followed by 45 cycles of 95 °C for 15 s and annealing at 60 °C for 30 s.

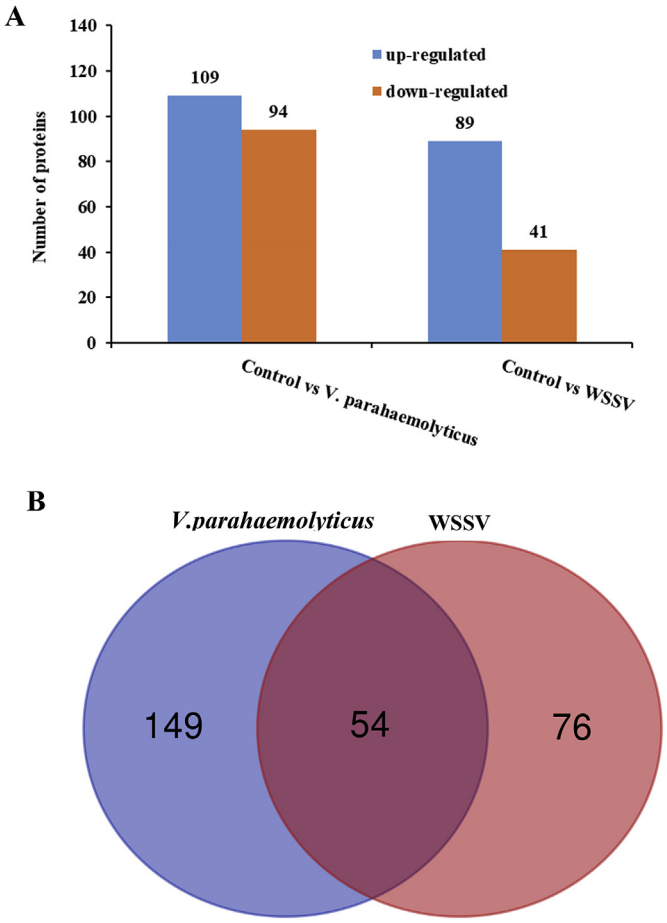

Fig. 1. The differentially abundant proteins were evaluated by IBT-based proteomics for relative and absolute quantitation analysis. (A) The numbers represent the proteins that were up-regulated or down-regulated (by more than 1.2-fold) compared with the *V. parahaemolyticus* and WSSV groups. (B) Venn diagram of differentially expressed abundant proteins.

2.7. Statistical analyses

The statistical analyses were carried out using SPSS 19.0 (IBM, Corp., Armonk, NY, USA). Data are presented as means ± the standard deviation (SD). Multiple comparison Tukey's tests were used to compare significant differences and the Shapiro–Wilk test was used to check data normality. $p < 0.05$ was considered significant.

3. Results

3.1. Proteomics overview

IBT analysis of *M. japonicas* hepatopancreas proteome resulted in 747,156 spectra being acquired, 56,955 of which were unique. From the LC–MS/MS spectra and peptide sequencing, 1005 proteins were identified (Table S2 **in the Supplementary Material**). The distribution of protein mass showed that 10% of the proteins had a mass > 100 kDa and 56% had a mass between 10 and 60 kDa in the identified proteome (Fig. S1 **in the Supplementary Material**).

GO enrichment analysis showed that 528 proteins could be annotated into the three major ontologies of biological processes, molecular functions, and cellular components (Fig. S2A **in the Supplementary Material**). The three most annotated biological process ontologies were catalytic activity (326), binding (197), and transporter activity (27).

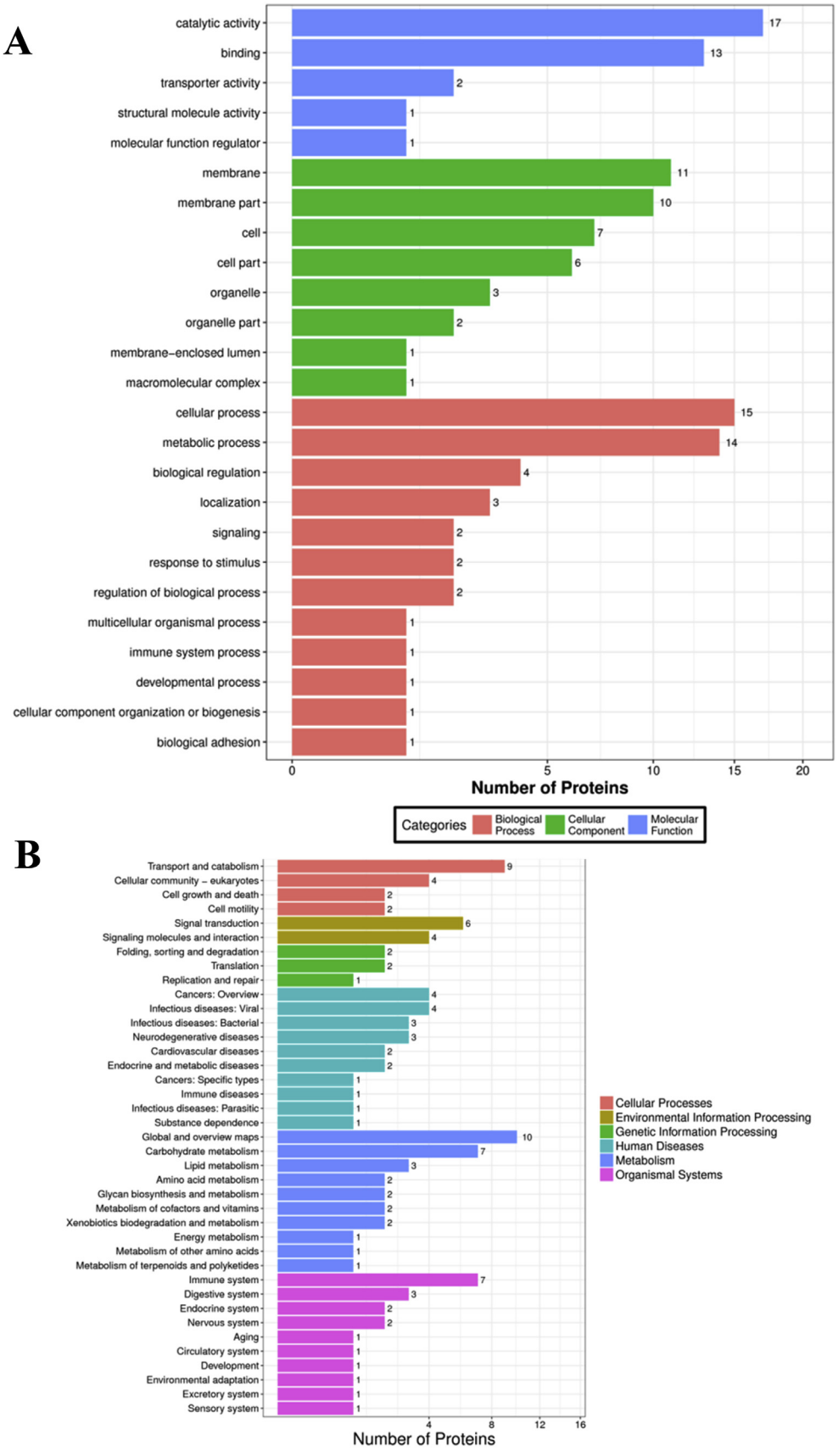

Fig. 2. Statistics of GO enrichment (A) and KEGG pathways (B) of differentially abundant proteins (more than 1.2-fold) in both *V. parahaemolyticus* and WSSV groups *vs.* the control group.

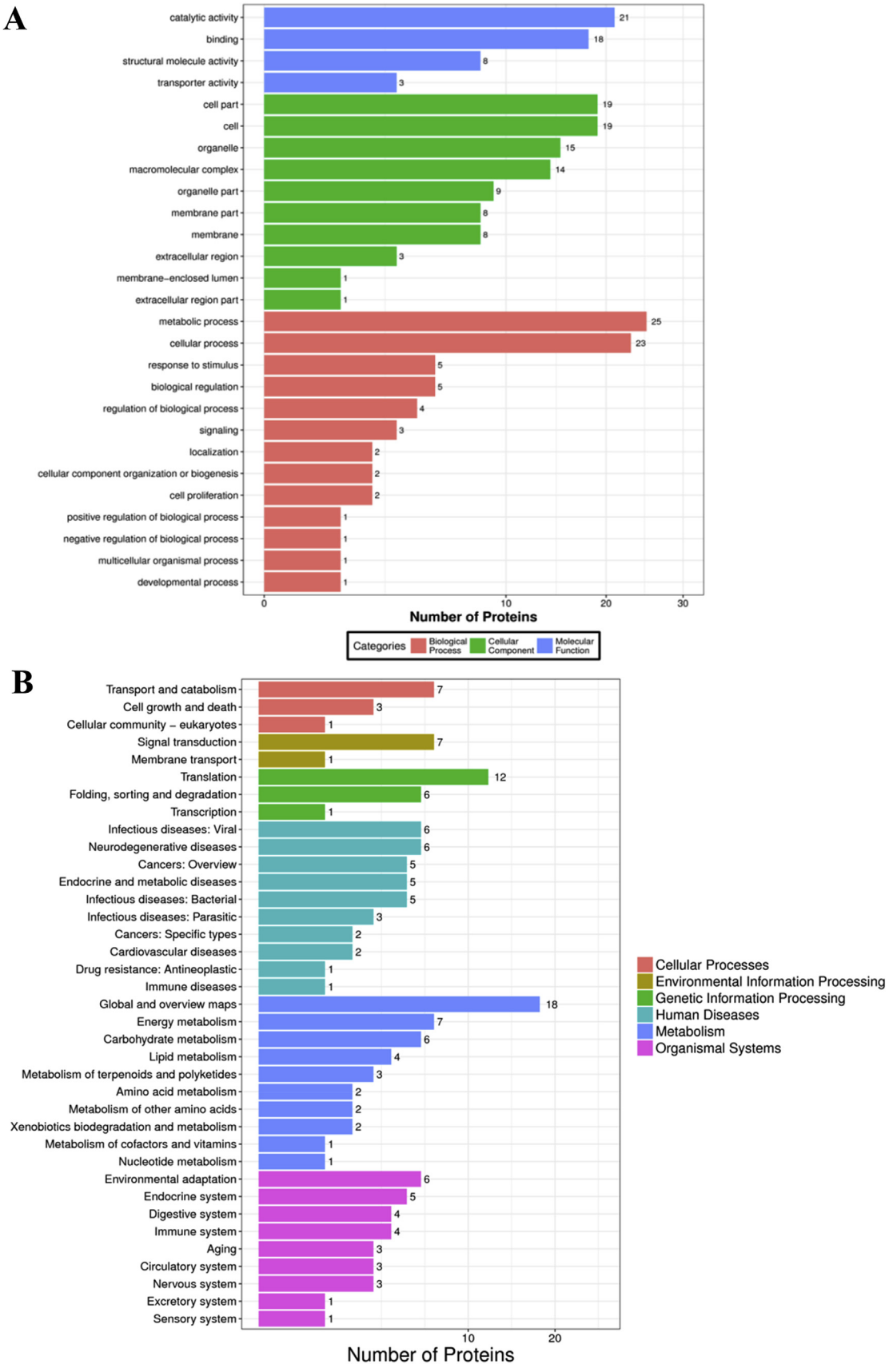

Fig. 3. Statistics of GO enrichment (A) and KEGG pathway (B) of differentially abundant proteins (more than 1.2-fold) from the *V. parahaemolyticus* group *vs.* the control group.

Table 1
The unique DAPs in the *M. japonicus* hepatopancreas during *V. parahaemolyticus* infection.

Protein name	Vibrio-*vs*.-control
Antigen processing and presentation	
Cathepsin D-like	1.67
Cathepsin B	1.96
Vitelline membrane outer layer protein 1 homolog	1.65
Vitelline membrane outer layer 1-like protein	1.78
Vitelline membrane outer layer protein 1	1.54
Proteasome subunit beta type-2-like	1.55
Nose resistant to fluoxetine protein 6 isoform X1	1.59
Huntingtin-interacting protein K-like	1.83
Cell adhesion molecules (CAMs)	
Pantetheinase-like	1.56
Mediator of RNA polymerase II transcription subunit	4.36
Putative glutamine-dependent NAD	1.53
Uncharacterized protein LOC107436837	1.62
Hypothetical protein DAPPUDRAFT_49503	1.72
Sphingomyelin phosphodiesterase-like	2.51
Hydroxyacylglutathione hydrolase, mitochondrial-like	1.88
Golgi apparatus protein	1.59
Mitochondrial import receptor subunit	1.74
Nucleoplasmin-like protein ANO39 isoform X2	1.74
Juvenile hormone esterase-like carboxylesterase 1	0.64
Alpha-N-acetylglucosaminidase isoform X1	0.59
Lactate dehydrogenase	0.56
Lysine histidine transporter 2-like	0.46
2-hydroxy-3-oxopropionate reductase-like-1	0.58
2-hydroxy-3-oxopropionate reductase-like	0.62
Cytoskeletal	
Uncharacterized protein LOC108682578	3.86
Actin	2.77
Rab14	1.54
JHE-like carboxylesterase 1	1.69
Molybdenum cofactor sulfurase-like isoform X1	1.53
Ubiquitin proteasome pathway	
Ubiquitin	2.13
E3 ubiquitin-protein ligase	1.52
Ring finger protein	1.54
Uncharacterized protein LOC108673556	1.57
Uncharacterized protein LOC108677414	2.81
Metabolic pathways	
Mitogen-activated protein kinase 1	3.92
Von Willebrand factor A domain-containing protein 7	1.74
Sodium bicarbonate transporter-like protein 11	2.87
Glucose transporter 2	3.94
Von Willebrand factor A domain-containing protein	1.68
ATP lipid-binding protein like protein	3.36
Map kinase-interacting serine	2.42
Copine-8	2.01
Acylpyruvase FAHD1, mitochondrial-like isoform X1	1.58
Uncharacterized protein LOC108667669	1.59
Uncharacterized protein LOC108669106	4.83
Proteinase and proteinases inhibitors	
Proteasome subunit beta type-7-like	1.78
Pyruvate carboxylase, mitochondrial-like	2.51
Retinol dehydrogenase 11-like	1.6
Glycine N-methyltransferase-like	1.54
Gamma-glutamyltranspeptidase 1-like isoform X1	1.68
Pacifastin light chain-like serine proteinase inhibitor	1.88
Rab GDP dissociation inhibitor alpha-like	1.55
Receptor-type tyrosine-protein phosphatase O	1.59
Argininosuccinate lyase-like isoform X1	1.65
Beta-galactosidase-1-like protein 2	1.88
Crustacyanin A1	2.07
60S acidic ribosomal protein P2-like protein	1.53
Uncharacterized protein LOC108670182	2.29
Uncharacterized protein LOC108673043	1.8
Carboxypeptidase B-like	2.11
Carboxypeptidase B-like-1	0.56
Eukaryotic translation initiation factor 4	0.53
Riken	0.63
Defender against apoptotic death	0.61
Proteasome alpha 3	0.64
Clathrin	0.65
Carboxypeptidase B	0.63
Calcineurin subunit A	0.55
Tight junction	
Actin-interacting protein 1-like isoform X2	1.56
Beta-1,3-glucan-binding protein precursor	2.25
Alpha-actinin-1-like	1.53
Sphingomyelin phosphodiesterase-like	1.54
Penlectin 5-3	1.75
Uncharacterized protein LOC108664581 isoform X4	1.78
Collagen alpha-5(IV) chain isoform X4	2.29
Beta-1,3-glucan-binding protein precursor	2.03
Phosphatidate cytidylyltransferase, photoreceptor	0.58
Gamma-butyrobetaine dioxygenase-like	0.63
Cell differentiation protein RCD1 homolog	0.64
Complement and coagulation cascades	
Alpha2-macroglobulin homolog	2.04
Alpha2 macroglobulin isoform 2	2.01
Trypsin-like serine proteinase	1.57
Putative serine protease	1.77
MAPK signaling pathway	
Sorbitol dehydrogenase	4.13
L-asparaginase 1-like	1.96
Uncharacterized protein LOC110848692	2.62
Uncharacterized protein LOC108674707	1.58
Neutral ceramidase-like	1.66
Microtubule-actin cross-linking factor 1 isoform X21	1.61
Calcium-activated chloride channel regulator 2	1.59
Aldehyde dehydrogenase family 16 member A1-like	1.57
SEC13 protein	2.14
Cysteine proteinase CG12163 isoform X4	2.08
Tubulin alpha-3 chain	0.53
Multidrug resistance-associated protein 1 isoform X7	0.59
Phospholipid-transporting ATPase ID isoform X4	0.66
Glutaryl-CoA dehydrogenase, mitochondrial	0.66
Phagosome	
C-type lectin 2	1.57
Fructose-bisphosphate aldolase-like	1.59
Vitellogenin	1.68
Chitinase-4	1.52
Hypothetical protein LOTGIDRAFT_203722	1.64
Uncharacterized protein APZ42_013126	1.53
Scavenger receptor class B, croquemort type	0.5
Nicotinamide phosphoribosyltransferase-like isoform X1	0.66
Sodium- and chloride-dependent taurine transporter protein	0.6
Sodium/bile acid cotransporter-like isoform X1	0.44
Organic cation transporter protein-like isoform X1	0.66
Alpha-I tubulin	0.61
Hypothetical protein DAPPUDRAFT_207744	0.65
Clarin-2-like isoform X1	0.57
Transmembrane emp24 domain-containing protein 2-like	0.62
Solute carrier family 22 member 24-like	0.64
Eukaryotic translation initiation factor 3 subunit E-B-like	0.5
EIF-2-alpha kinase activator GCN1-like	0.62
Sodium/bile acid cotransporter-like isoform X1	0.61
Solute carrier family 43 member 3-like	0.55
Splicing factor 3B subunit 1-like isoform X1	0.63
Slow-tonic S2 tropomyosin	0.43
Drop dead	0.64
Adenine nucleotide translocase 2	0.52
Elongation factor 1-alpha	0.64
Hypothetical protein T11_10141	0.52
Low-density lipoprotein receptor-related protein 2-like	0.43
S-methyl-5′-thioadenosine phosphorylase-like protein	0.52
Protein pelota	0.55
3-hydroxyisobutyryl-CoA hydrolase	0.62
Acid phosphatase	0.51
Persulfide dioxygenase ETHE1	0.53
Pattern Recognition Proteins	
Lectin B isoform 2	0.61
Acetyl-coenzyme A synthetase	0.61
Regulation of actin cytoskeleton	0.51
Oplophorus-luciferin 2-monooxygenase non-catalytic	0.59
Juvenile hormone esterase-like carboxylesterase 1	0.63
Scavenger receptor B	0.66
Hypothetical protein DAPPUDRAFT_230571	0.53
Uncharacterized protein LOC108672784	0.63

(*continued on next page*)

Table 1 (*continued*)

Protein name	Vibrio-*vs*.-control
Toll-like receptor 1	0.63
Estrogen sulfotransferase-like	0.66
Low affinity cationic amino acid transporter 2	0.61
40S ribosomal protein S3-like	0.56
Fucose mutarotase-like	0.64
Endonuclease-reverse transcriptase	0.55
Ribonuclease Oy-like isoform X3	0.62
Basic proline-rich protein-like	0.52
Peroxisome	
Invertebrate-type lysozyme protein	0.56
GST-N-Metaxin-like protein	0.6
Cytochrome P450 2L1	0.58
Translocating chain-associated membrane protein	0.63
DDX6	0.61

The three most annotated cellular component ontologies wre membrane (206), membrane part (191), and cell (177). The three most annotated molecular function ontology included metabolic progress (216), cellular progress (201), and biological regulation (51).

In addition, cluster of orthologous groups (KOG) analysis mapped and classified the 528 proteins into four KOG sub-group: Cellular processes and signaling, information storage and processing, metabolism, and poorly characterized (Fig. S2B **in the Supplementary Material**). KEGG analysis annotated the 528 proteins into six major KEGG pathways: Cellular processes, environmental information processing, genetic information processing, human diseases, metabolism, and organismal systems. The annotated proteins could then be divided into 44 level 2 subcategories pathways. The largest subcategory group was global overview maps, which had 285 annotated proteins, followed by transport and catabolism (131), carbohydrate metabolism (121) and signal transduction (94), etc. (Fig. S2C **in the Supplementary Material**).

3.2. GO and KEGG analysis of DAPs

To identify DAPs among the identified proteins we use thresholds of a 1.2-fold ($p < 0.05$) increase or a 0.83-fold decrease to identify proteins that underwent a physiologically relevant change in abundance. Among the identified proteins, 213 were identified as DAPs, of which 109 were upregulated and 94 were downregulated after *V. parahaemolyticus* challenge (Fig. 1A). Similarly, 130 proteins were identified as DAPs after WSSV challenge, of which 88 were upregulated and 42 were downregulated. Thus, in the shrimp hepatopancreas, *V. parahaemolyticus* infection affected protein to a greater extent than WSSV infection. Under both challenges, there were more upregulated than downregulated proteins. Among the DAPs, 54 proteins were significantly up- or downregulated under challenge with *V. parahaemolyticus* and WSSV (Fig. 1B), suggesting that these DAPs might take part in the shrimp immune response to WSSV infection, *V. parahaemolyticus*, or both. GO analysis indicated that the main molecular functions of the DAPs binding, catalytic activity, and organelle components (Fig. 2A). The 54 DAPs appeared to be associated with important pathways such as ribosome, mitogen-activated protein kinase (MAPK) signaling, carbon metabolism phagosome, hippo signaling, and Ras signaling (Fig. 2B).

For the DAPs identified after *V. parahaemolyticus* challenge, the GO analysis showed that catalytic activity and cellular process were the most important categories (Fig. 3A). KEGG enrichment indicated that carbohydrate metabolism was the most important subcategory (Fig. 3B). The upregulated proteins were grouped into ten functions, which included antigen processing and presentation, cell adhesion molecules (CAMs) and the cytoskeleton. The downregulated proteins were grouped into nine functions, which included CAMs, the MAPK signaling pathway, proteinase, and proteinases inhibitors. (Table 1).

For the DAPs identified after WSSV challenge, the GO analysis showed that metabolic process and cellular process were the most important categories. KEGG enrichment indicated that translation was the most important category (Fig. 4). The upregulated proteins were grouped into nine functions, which included antigen processing and presentation, CAMs, cytoskeleton, and phagosome. The data identified that many phagosome, cytoskeleton, and endocytosis-related proteins from the hepatopancreas may be associated with WSSV infection. The downregulated DAPs were grouped into six functions, which included CAMs, protein and proteinase, tight junction, metabolic pathways, phagosome, and other proteins (Table 2).

Interestingly, certain proteins showed significant ($p < 0.05$) changes in abundance after challenge with both *V. parahaemolyticus* and WSSV infection (Table 3). The upregulated proteins could be grouped into seven functions, including CAMs, tight junction, and cell death. The downregulated proteins could also be grouped into seven functions, including phagosome, MAPK signaling pathway, antigen processing and presentation, metabolic pathways, tight junction, peroxisome, and other proteins.

3.3. Verification using quantitative real-time polymerase reaction (qPCR)

To verify the IBT data, we selected ten DAPs and used qPCR to assess their mRNA expression levels in the shrimp hepatopancreas after pathogen challenge (Fig. 5). Among the 10 selected DAPs, two upregulated DAPs (α_2-M and chitinase-4) and two downregulated DAPs (scavenger receptor B and toll-like receptor) were expressed only in *V. parahaemolyticus*-infected group, two upregulated DAPs (alpha actin and GST) and two downregulated DAPs (C-type lectin and triosephosphate isomerase) were expressed only in WSSV-infected group; and two upregulated DAPs (integrin and caspase-3) were expressed in both the *V. parahaemolyticus* and WSSV-infected groups were used for transcriptional detection. The qPCR analysis showed that all selected candidates proteins presented the same transcriptional expression trends as their protein level trends except for scavenger receptor B expressed in WSSV-infected group. The mRNA expression of scavenger receptor B was upregulated, while the protein expression was downregulated. Although this gene showed a reverse expression pattern at the protein and mRNA levels, it is not uncommon for the transcript levels of a gene to not match the levels of their corresponding protein because the abundance of a protein depends not only on the transcript level, but also on post-translational modifications and processes.

4. Discussion

The hepatopancreas is an important organ involved in crustacean innate immunity [14–16], digestive enzymes synthesis [17], and nutrient absorption and storage [18]. The present study used the IBT-based proteomics method to determine the proteomic profiles of the *M. japonicus* hepatopancreas after *V. parahaemolyticus* and WSSV challenge. The results demonstrated significant alterations in the levels of various proteins and their associated biological processes in the hepatopancreas after bacteria and virus challenge. IBT analysis identified 1005 proteins in the *M. japonicus* hepatopancreas proteome, 56% of which had a mass between 10 and 60 kDa. Major pathways analysis identified 285 proteins in the global overview maps category, 131 in the transport and catabolism category, and 94 in the signal transduction category. In the GO category of biological processes, catalytic activity and binding were the major subcategories, and in the category molecular functions, the major subcategories were metabolic progress and cellular progress.

4.1. The differentially abundant proteins in response to V. parahaemolyticus challenge

Among 82 upregulated proteins, several proteins (e.g., chitinase-4,

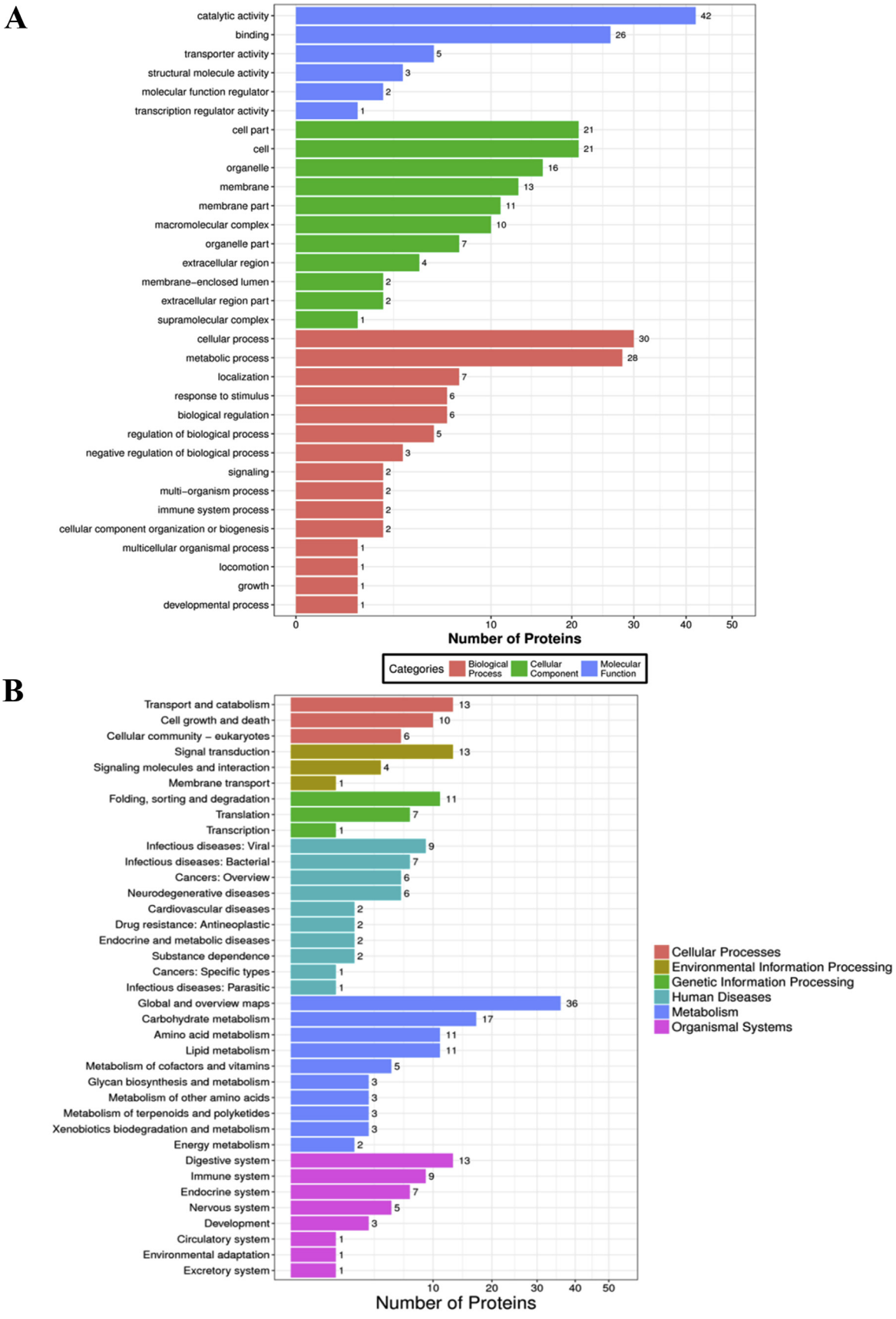

Fig. 4. Statistics of GO enrichment (A) and KEGG pathway (B) of differentially abundant proteins (more than 1.2-fold) from the WSSV group *vs.* the control group.

Table 2
The unique DAPs in the *M. japonicus* hepatopancreas during WSSV infection.

Protein name	WSSV-*vs.*-control	
Antigen processing and presentation		
Heat shock 70 kDa protein cognate 5	2.2	
Heat shock protein 70	2.1	
Calreticulin	1.82	
Hypothetical protein DAPPUDRAFT_303875	1.85	
Hypothetical protein AMK59_6238	1.68	
Uncharacterized protein LOC100376424	2.43	
Cell adhesion molecules (CAMs)		
Hemocyanin subunit Y	1.79	
Iron regulatory protein 1-like protein	1.58	
Feline leukemia virus subgroup C receptor-related protein	1.55	
Elongation factor 1-delta protein	1.63	
crustin-like peptide	1.81	
Glucan pattern-recognition lipoprotein	1.74	
Arylsulfatase D-like	0.62	
Integrin beta subunit		0.52
Complement and coagulation cascades		
Filaggrin-2-like isoform X3		2.32
14-3-3-like protein		1.53
Tail muscle elongation factor 1 gamma		1.59
Cytoskeletal		
Alpha actin		2.69
Protein SET-like		1.56
Myosin light chain		1.67
Myosin heavy chain		1.69
Phagosome		
Mannose-binding protein		1.58
Calumenin-B-like		1.54
Protein farnesyltransferase/geranylgeranyltransferase		1.55
C-type lectin		0.61
Retinoid-inducible serine carboxypeptidase-like		0.58
Cell death		
Mitochondrial ubiquinol-cytochrome c reductase protein		1.65
Ferritin		1.67
Hypothetical protein DAPPUDRAFT_207426		1.52
Putative carnitine O-acetyltransferase		1.52
Betaine–homocysteine S-methyltransferase 1-like		2.4
Tight junction		
Acyl-CoA-binding protein		1.6
ADP ribosylation factor 4		1.52
Ribonuclease UK114-like		1.79
Glucose-6-phosphate isomerase		1.87
Glycosyl-phosphatidylinositol-linked carbonic anhydrase		2.24
Protein disulfide isomerase 2		1.57
Carboxypeptidase B-like		4.3
Succinate dehydrogenase [ubiquinone] iron-sulfur		1.67
GTP binding protein alpha subunit Gq		1.91
Sialin-like		0.66
Peritrophin-44-like protein		0.58
Metabolic pathways		
F0-ATP synthase b-chain		2.98
ATP-binding cassette sub-family B member 7		1.83
Flavin reductase (NADPH)-like		1.86
Long-chain specific acyl-CoA dehydrogenase		1.76
Phosphoglucomutase-2-like		1.63
Phosphopyruvate hydratase		2.29
Triosephosphate isomerase		0.49
Chiniase 3		0.52
Oxidative stress		
Glutathione S-transferase		2.09
NADH dehydrogenase		2.28
Thioredoxin reductase		1.66
Protein and proteinase		
60S ribosomal protein L31		0.59
Juvenile hormone epoxide hydrolase		0.55
Dehydrogenase/reductase SDR family member		0.62
Vitelline membrane outer layer protein 1		0.64
Phospholipase D gamma 3-like		0.56
Putative protein phosphatase		0.6
Proteinase and proteinases inhibitors		
Prostaglandin reductase 1-like		1.83
Sphingosine-1-phosphate lyase-like		2.64
Eukaryotic translation initiation factor 4 gamma		1.72
Ribosomal protein L3		1.53
Ribosomal protein L9		1.77
Ribosomal protein L35		1.71
40S ribosomal protein S5		1.69
40S ribosomal protein S4		2.43
60S ribosomal protein L17		2.54
60s ribosomal protein l27a		1.72
60S ribosomal protein L35a		1.52
60S ribosomal protein L11-like		2.55
60S ribosomal protein L14 isoform X1		1.59
Sphingomyelin phosphodiesterase-like		1.83
Other proteins		
Uncharacterized protein LOC108682883		0.66
Uncharacterized protein LOC108673189		0.61
Cuticular protein analogous to peritrophins		0.65

tachylectin and α_2M) were related to bacterial infection and host immunity. Chitinase can directly kill invading pathogens by degrading their chitin-containing structures, constituting an important part of the host defense [19], and its expression profile upon *V. parahaemolyticus* infection was also consistent with the results of a previous study [20]. In the present study, the expression of tachylectins after *M. japonicus* infection was upregulated. This results seemed to suggest that the host attempted to clear the infection upon receiving the bacterial injection, by upregulating tachylectins expression. Alpha2-macroglobulin (α_2-M) is a member of ungrouped proteins, whose best-characterized function is the control and regulation of the prophenoloxidase (proPO)-activating system to avoid any deleterious effects to of infection in crustaceans [21]. There was a report that α_2-M might assist the phagocytosis activating protein (PAP) to enter into phagocytic cells, to decrease the mortality of shrimp after challenge with WSSV [22]. In our study, the transcript and protein levels of α_2-M was downregulated post infection.

Among 67 downregulated proteins, the pattern recognition proteins (PRPs) including scavenge receptor B (SR-B) and toll-like receptor (TLR) wre prominent. These proteins play an important role by recognizing and binding to common epitopes on the pathogen surface such as β-1,3-glucans (BGs), lipopolysaccharides (LPSs), and peptidoglycans (PGs) [23,24]. Thus, SR-B and TLR of *M. japonicus* may be the receptors for *V. parahaemolyticus* binding. As such, reducing their abundance might help the host cells resist invasion by the bacteria. Although the mRNA levels of SR-B did not match the protein expression levels perfectly, there are many post-translational processes that could affect the levels of a protein within the cell [25]. Knockdown of the SR-B gene led to a decrease the mortality rate and an increase in infection time in *V. anguillarum*-infected *M. japonicus* [23].

4.2. The differentially abundant proteins in response to WSSV challenge

The proteomic profiles of the hepatopancreas between the control and WSSV infected *M. japonicus* were successfully constructed to reveal the DAPs that responded to infection. Among 59 upregulated proteins, heat shock protein 70, crustin hemocyanin, and 14-3-3 protein were reported to be involved with anti-white spot syndrome virus peptides. Heat shock proteins (HSPs) play important roles in stress tolerance and promote cell survival through refolding proteins and preventing proteins denaturation [26]. We speculated that the upregulation of HSP70 might help the hepatopancreas to reduce the cell damage caused by WSSV infection. Furthermore, the increased level of HSP 70 was also found in total haemocytes of *F. chinensis* during WSSV infection [27], which implied its important role in WSSV infection. Crustin was reported to be involved with anti-white spot syndrome virus peptides. They were upregulated in the haemocytes of WSSV-infected *P. monodon* [28]. Knockdown crustin by RNAi led to a higher level of WSSV propagation, suggesting a crucial role of crustin as a regulator of WSSV

Table 3
Differentially abudant proteins in the *M. japonicus* hepatopancreas in both *V. parahaemolyticus* and WSSV infection groups.

Protein name	Vibrio-VS-control	WSSV-VS-control
Cell adhesion molecules (CAMs)		
Integrin beta subunit	2	1.59
Vascular endothelial growth factor receptor precursor	1.7	1.61
Complement and coagulation cascades		
Alpha2-macroglobulin homolog	2.11	2.51
Hypothetical protein DAPPUDRAFT_330735	1.79	2.6
Uncharacterized protein LOC108674546	1.59	1.87
Tight junction		
Ferritin	2.02	2.27
Hypothetical protein DAPPUDRAFT_315834	1.51	1.76
Annexin B9-like isoform X4	2.35	2.13
Annexin B9-like isoform X4	2.65	1.95
Proteinase and proteinases inhibitors		
Lysosomal alpha-mannosidase-like	2.25	1.69
Hemocyte kazal-type proteinase inhibitor	2.14	1.55
60S ribosomal protein L34	1.66	3.52
Serine proteinase inhibitors	1.62	1.6
Cell death		
Caspase 3	1.52	1.53
Inhibititor of apoptosis protein	2.1	1.51
Mitochondrial cytochrome c1	3.13	1.95
Metabolic pathways		
Glyceraldehyde-3-phosphate-dehydrogenase	2.46	2.01
Liver carboxylesterase 1-like	2.43	3.59
Fatty-acid amide hydrolase 2-like	1.99	1.59
Uncharacterized protein APZ42_013126	1.54	1.64
Failed axon connections homolog	1.83	1.59
Gamma-interferon induced thiol reductase GILT3	1.94	1.52
Ribose-5-phosphate isomerase-like	2.26	2.25
Hypothetical protein BRAFLDRAFT_126490	1.65	1.85
MAPK signaling pathway		
Succinate dehydrogenase [ubiquinone] flavoprotein s	2.68	1.59
Ubiquitin carboxyl-terminal esterase L3	1.79	3.01
Lysosomal alpha-mannosidase-like	1.95	1.61
Phagosome		
C-type lectin	0.54	0.62
D-beta-hydroxybutyrate dehydrogenase	0.52	0.59
Antigen processing and presentation		
Cathepsin A	0.66	0.64
Choline transporter-like protein 2	0.65	0.65
Secernin-2-like isoform X2	0.55	0.56
Dipeptidase 1-like	0.62	0.62
MAPK signaling pathway		
Serine/threonine protein phosphatase 1	0.62	0.62
Metabolic pathways		
Uncharacterized protein LOC108664398	0.55	0.55
Dystroglycan	0.57	0.6
ATP-citrate synthase-like isoform X1	0.61	0.64
Dimethylglycine dehydrogenase, mitochondrial-like	0.64	0.53
Tight junction		
GTP-binding protein	0.57	0.62
Talin-1	0.63	0.66
Oplophorus-luciferin 2-monooxygenase non-catalytic	0.51	0.61
2-acylglycerol O-acyltransferase 1-like	0.54	0.63
Chymotrypsin BII; Flags: Precursor	0.54	0.62
PMAV	0.54	0.52
Mitochondrial dicarboxylate carrier-like	0.65	0.61
Peroxisome		
Cytosolic MnSOD	0.58	0.59
Putative oxidoreductase YteT isoform X1	0.59	0.54
Trimethyllysine dioxygenase	0.59	0.58
Other proteins		
Sorting nexin-6	0.48	0.5
Uncharacterized protein ZK1073.1-like isoform X3	0.66	0.61
Chymotrypsin	0.66	0.66
Vitelline membrane outer layer 1-like protein	0.64	0.54
Peritrophin	0.42	1.87
Isocitrate dehydrogenase [NADP] cytoplasmic-like	0.63	1.58

replication [29]. Hemocyanin functions as an immunoglobulin superfamily molecule and is one of the important host factors against viruses invasion [30]. In the present study, the level of hemocyanin after *M. japonicus* infection was upregulated. Virus infection-related upregulation of hemocyanin has been investigated previously at transcriptional and protein level [8]. The 14-3-3 protein is a member of ungrouped proteins identified upon WSSV infection, which plays important roles in metabolism, cell cycle, cell growth, cell survival and apoptosis [31]. In the present study, the increased protein level of 14-3-3 suggested an ssociation with WSSV infection in *M. japonicas*.

Among 17 downregulated proteins, C-type lectin mediates the immune mechanism by recognizing the pathogen and is involving in cell-cell interactions [32]. WSSV-infection *M. japonicas* resulted in immune-suppressive and adverse effects on the hosts thorough inhibition of C-type lectin-mediated immune responses; regulation of the complement and coagulation pathway; dysregulation of important cell adhesion molecules and the extracellular matrix; and imbalance of the cellular redox homeostasis in the hepatopancreas of the affected shrimps. Triosephosphate isomerase plays an important role in several metabolic pathways and is essential for efficient energy production [33]. In this study, the key glycolytic enzyme, triosephosphate isomerase, was downregulated after WSSV challenge. Triosephosphate isomerase was also downregulated in the hepatopancreas of *F. chinensis* post-WSSV infection [34]. The decrease levels of these immune responsive proteins revealed the major role of the hepatopancreas as a defensive tissue against WSSV infection.

4.3. The same DAPs and pathways in response to V. parahaemolyticus or WSSV challenge

Among the proteins affected by both WSSV and *V. parahaemolyticus* challenge, GO analysis showed that cellular process and metabolic process were the most important GO categories, and that global overview maps was the key pathway. WSSV and *V. parahaemolyticus* challenge both altered the levels the same 54 proteins. The important pathways associated with these common DAPs included ribosome pathways, the MAPK signaling pathway, carbon metabolism pathways, phagosome pathways, and the Ras signaling pathway. Cellular process, metabolic process, and biological regulation were the major molecular functions associated with these DAPs.

Among the 54 DAPs, the anti-lipopolysaccharide factors (ALF) are the most widespread effectors that affect invading microorganisms in crustaceans and are involved in antimicrobial activity that kills gram-positive, gram-negative bacteria, and viruses [35,36]. Our results showed that ALF3 was upregulated in response to both WSSV and *V. parahaemolyticus* challenge, demonstrating its importance as a defense molecule against pathogens. Ferritin is an iron storage protein that is vital for the cellular metabolism of iron and to maintain iron homeostasis [37]. Ferritin was activated in the transcriptome of the shrimp *Macrobrachium rosenbergii* post *V. parahaemolyticus* infection [38], which agreed with the results of our proteomic analyses. Integrin, which mediates cell-to-extracellular matrix, cell-to-cell, and cell-to-pathogen interactions [39], was activated in response to challenge by both pathogens. Integin was also activated during WSSV infection of *F. chinensis* [40].

In response to *V. parahaemolyticus* and WSSV infection, cells can undergo apoptosis via several mechanisms, including via pore-forming

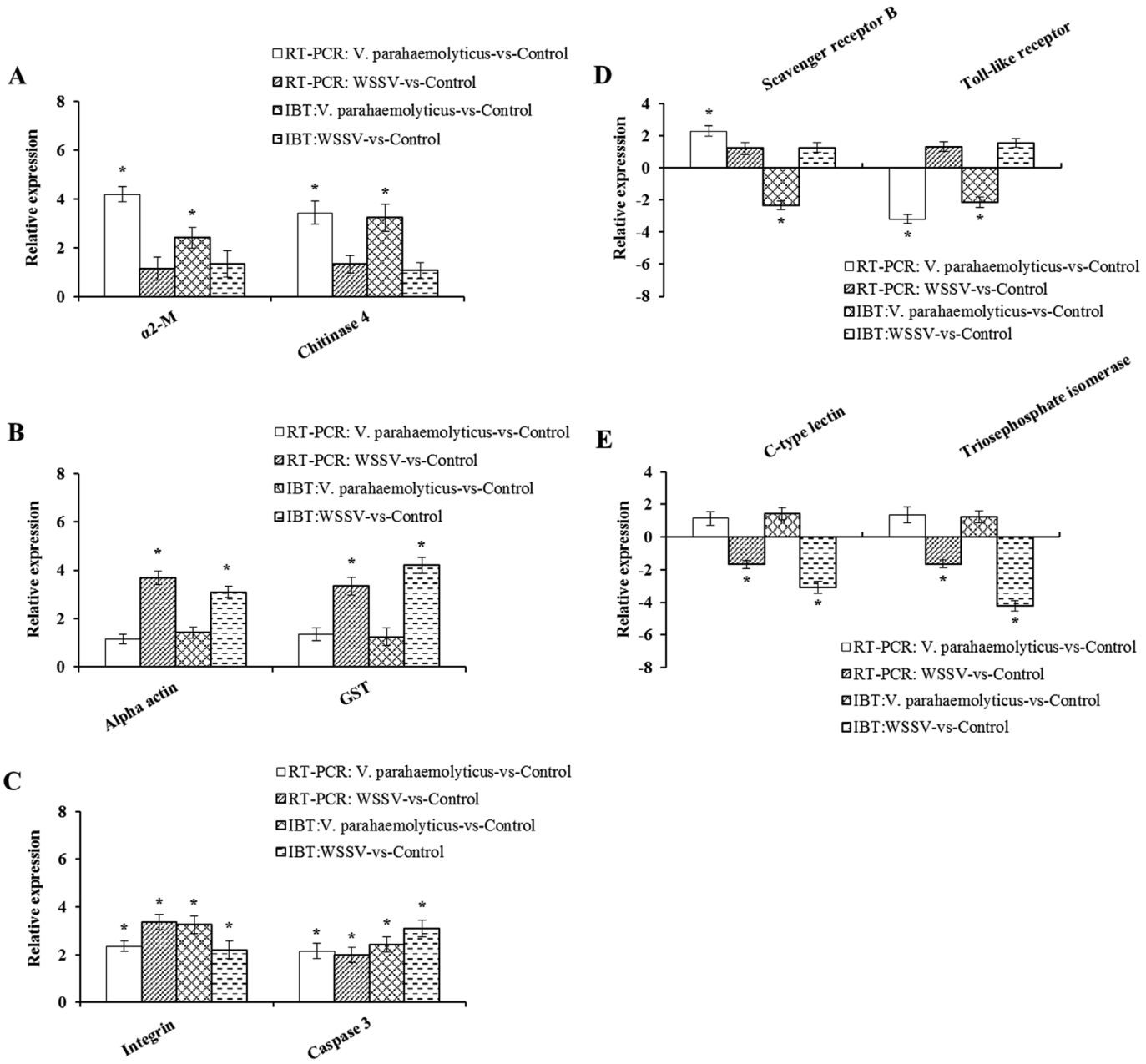

Fig. 5. Protein and mRNA expression levels of the differentially expressed genes detected using real-time PCR. Asterisks on the graph denote statistically significant differences ($p < 0.05$).

proteins, and the secretion of protein synthesis inhibitors, molecules that activate the endogenous death machinery, lipopolysaccharides, or other superantigens [41]. Increased shrimp mortality may be caused by increased apoptosis-related degradation of DNA and RNA [42]. Our proteomic data showed upregulation of apoptosis-related mitochondrial cytochrome *c*1 and caspase 3, which was similar to the results of a previous study [47]. Apoptosis could also function in host defense against pathogens by permitting phagocytosis of apoptotic bodies containing pathogens by healthy cells to effectively clear the pathogen [43].

4.4. The different DAPs and pathways in response to V. parahaemolyticus or WSSV challenge

V. parahaemolyticus infection damages the mitochondria in cells of hepatopancreas, ultimately resulting in the death of shrimp [44]. By contrast, WSSV infection induces metabolic changes [45], and in crustaceans, its replication is dependent on endocytosis [46]. We identified many DAPs between *V. parahaemolyticus* and WSSV. However, the numbers of up and downregulated proteins were different between the two challenges. After, *V. parahaemolyticus* infection, 149 DAPs were significantly up- or downregulated, whereas during WSSV infection, 76 DAPs were significantly up- or downregulated. Thus, similar to a previous report [9], infection with *V. parahaemolyticus* had a significant effect on more proteins than did WSSV infection.

Among the DAPs induced by *V. parahaemolyticus* infection, high expression of certain tight junction proteins was noted, such as beta-1,3-glucan-binding protein, actin-interacting protein, and penlectin, which have vital functions in cell division, cell growth, and recognition signaling pathways [46]. *V. parahaemolyticus* challenge caused the upregulation of six phagosome-related proteins. Upregulation of vitellogenin and chitinase-4, which have important functions in many cellular

processes, such as phagocytosis, nodule formation, encapsulation, cell motility, adhesion, and cell shape change, might enhance clearing of gram-positive bacteria [47].

WSSV infection resulted in altered levels of many cytoskeleton proteins, which suggested that phagocytosis is an important cellular process during infection, as noted in previous reports [48]. In shrimp, phagocytosis is regulated by actin and myosin, which also participate in the response to WSSV [49,50]. In invertebrates, phagocytosis is a major immune response to virus challenge. Our results showed significant upregulation of alpha actin and myosin ($p < 0.05$) in response to WSSV challenge, which indicate that these two proteins play important roles in the immune response. Similarly, in *L. vannamei*, the cytoskeleton and actin regulation were significantly associated with WSSV infection [51].

Oxygen radical concentrations are regulated by the activities of antioxidant enzymes. For example, xenobiotics are marked for cellular degradation by glutathione-S-transferase (GST) [52], and pathogen infection usually increases this antioxidant activity. Our results showed that in the *M. japonicus* hepatopancreas, GST levels were obviously increased upon WSSV infection. Similarly, WSSV infection resulted in upregulated GST protein levels in the claw crayfish, *Cherax quadricarinatus* [53]. During infection, when the rate of free radical formation exceeds that of its removal by the antioxidant system, increased oxidative damage will occur [54]. Cell death can occur because of defects in antioxidant defense that fail to protect sensitive cellular and subcellular components [55]. Taken together, these findings demonstrated that in crustaceans, WSSV infection modulates the antioxidant response.

5. Conclusions

In the present study, we determined the hepatopancreas proteome of *M. japonicus* after challenge with WSSV and *V. parahaemolyticus*. After *V. parahaemolyticus* challenge, 109 proteins were significantly upregulated, and 94 were significantly downregulated. After WSSV challenge, 88 proteins were significantly upregulated and 42 were significantly downregulated. Among them, 54 proteins were differentially abundant after both *V. parahaemolyticus* and WSSV challenge. We used the proteomic data to further analyze the immune response of *M. japonicus* during pathogen infection. These results will increase our understanding of the molecular mechanisms of shrimp's immune response to *V. parahaemolyticus* or WSSV infection.

Declarations of interest

None.

Acknowledgments

This work was supported by the Projects of International Exchange and Cooperation in Agriculture, Ministry of Agriculture and Rural Affairs of China- Science, Technology and Innovation Cooperation in Aquaculture with Tropical Countries, and the Program of Shandong Leading Talent [grant number LNJY2015002]. We thank the staff at the Key Laboratory for Sustainable Utilization of Marine Fisheries Resources for their help with sampling and maintaining the shrimp.

Appendix A. Supplementary data

Supplementary data to this article can be found online at https://doi.org/10.1016/j.fsi.2019.08.039.

References

[1] S. Zhong, Y. Mao, J. Wang, M. Liu, M. Zhang, Y. Su, Transcriptome analysis of kuruma shrimp (*Marsupenaeus japonicus*) hepatopancreas in response to white spot syndrome virus (WSSV) under experimental infection, Fish Shellfish Immunol. 70 (2017) 710–719.
[2] Bureau of Fisheries, Ministry of Agriculture, P.R.C, Fisheries economic statistics, China Fishery Yearbook, vol. 238, China Agricultural Press, Beijing, 2018.
[3] X. Zhang, G. Li, H. Jiang, L. Li, J. Ma, H. Li, J. Chen, Full-length transcriptome analysis of *Litopenaeus vannamei* reveals transcript variants involved in the innate immune system, Fish Shellfish Immunol. 87 (1) (2019) 346–359.
[4] A. Tassanakajon, K. Somboonwiwat, P. Supungul, S. Tang, Discovery of immune molecules and their crucial functions in shrimp immunity, Fish Shellfsh Immunol 34 (2013) 954–967.
[5] A. Tassanakajon, K. Somboonwiwat, P. Supungul, S. Tang, Discovery of immune molecules and their crucial functions in shrimp immunity, Fish Shellfsh Immunol 34 (2013) 954–967.
[6] C.Y. Xie, J.R. Kong, C.S. Zhao, Y.C. Xiao, T. Peng, Y. Liu, W.N. Wang, Molecular characterization and function of a PTEN gene from *Litopenaeus vannamei* after *Vibrio alginolyticus* challenge, Dev. Comp. Immunol. 59 (2016) 77–88.
[7] S.H. Li, F.H. Li, Z. Sun, X.J. Zhang, J.H. Xiang, Differentially proteomic analysis of the Chinese shrimp at WSSV latent and acute infection stages by iTRAQ approach, Fish Shellfish Immunol. 54 (2016) 629–638.
[8] A. Hernández-Pérez, J.A. Zamora-Briseño, E. Ruiz-May, A. Pereira-Santana, J.M. Elizalde-Contreras, S. Pozos-González, R. Rodríguez-Canul, Proteomic profiling of the white shrimp *Litopenaeus vannamei* (Boone, 1931) hemocytes infected with white spot syndrome virus reveals the induction of allergy-related proteins, Dev. Comp. Immunol. 91 (2019) 37–49.
[9] B. Sun, Z. Wang, Z. Wang, X. Ma, F. Zhu, A proteomic study of hemocyte Proteins from mud crab (*Scylla paramamosain*) infected with White spot syndrome Virus or *Vibrio alginolyticus*, Front. Immunol. 8 (2017) 468.
[10] S.V. Durand, D.V. Lightner, Quantitative real time PCR for the measurement of white spot syndrome virus in shrimp, J. Fish Dis. 25 (7) (2002) 381–389.
[11] X.P. Li, X.H. Meng, J. Kong, K. Luo, S. Luan, B. Cao, X.L. Shi, Identification, cloning and characterization of an extracellular signal-regulated kinase (ERK) from Chinese shrimp, *Fenneropenaeus chinensis*, Fish Shellfish Immunol. 35 (6) (2013) 1882–1890.
[12] L.L. Xing, L.N. Sun, S.L. Liu, X.N. Li, L.B. Zhang, H.S. Yang, IBT-based quantitative proteomics identifies potential regulatory proteins involved in pigmentation of purple sea cucumber, *Apostichopus japonicus*, Comp. Biochem. Physiol. D 23 (2017) 17–26.
[13] X.Y. Ren, P. Liu, J. Li, Comparative transcriptomic analysis of *Marsupenaeus japonicus* hepatopancreas in response to *Vibrio parahaemolyticus* and white spot syndrome virus, Fish Shellfish Immunol. 87 (2019) 755–764.
[14] T. Rőszer, The invertebrate midintestinal gland ("hepatopancreas") is an evolutionary forerunner in the integration of immunity and metabolism, Cell Tissue Res. 358 (3) (2014) 685–695.
[15] L.S. Dai, M.N. Abbas, S. Kausar, Y. Zhou, Transcriptome analysis of hepatopancreas of *Procambarus clarkii* challenged with polyriboinosinic polyribocytidylic acid (poly I: C), Fish Shellfish Immunol. 71 (2017) 144–150.
[16] M. Zhou, M.N. Abbas, S. Kausar, C.X. Jiang, L.S. Dai, Transcriptome profiling of red swamp crayfish (*Procambarus clarkii*) hepatopancreas in response to lipopolysaccharide (LPS) infection, Fish Shellfish Immunol. 71 (2017) 423–433.
[17] G. Vogt, Life-cycle and functional cytology of the hepatopancreatic cells of *Astacus astacus* (Crustacea, Decapoda), Zoomorphology 114 (2) (1994) 83–101.
[18] F. Li, J. Xiang, Recent advances in researches on the innate immunity of shrimp in China, Dev. Comp. Immunol. 39 (1–2) (2013) 11–26.
[19] S. Niu, L. Yang, H. Zuo, J. Zheng, S. Weng, J. He, X. Xu, A chitinase from pacific white shrimp *Litopenaeus vannamei* involved in immune regulation, Dev. Comp. Immunol. 85 (2018) 161–169.
[20] Y. Sun, J. Zhang, J. Xiang, A CRISPR/Cas9-mediated mutation in chitinase changes immune response to bacteria in *Exopalaemon carinicauda*, Fish Shellfsh Immunol 71 (2017) 43–49.
[21] S. Ponprateep, T. Vatanavicharn, C.F. Lo, A. Tassanakajon, V. Rimphanitchayakit, Alpha-2-macroglobulin is a modulator of prophenoloxidase system in pacific white shrimp *Litopenaeus vannamai*, Fish Shellfsh Immunol 62 (2017) 68–74.
[22] H. Ma, B. Wang, J. Zhang, F. Li, J. Xiang, Multiple forms of alpha-2 macroglobulin in shrimp *Fenneropenaeus chinensis* and their transcriptional response to WSSV or *Vibrio* pathogen infection, Dev. Comp. Immunol. 34 (2010) 677–684.
[23] W.J. Bi, D.X. Li, Y.H. Xu, S. Xu, J. Li, X.F. Zhao, J.X. Wang, Scavenger receptor B protects shrimp from bacteria by enhancing phagocytosis and regulating expression of antimicrobial peptides, Dev. Comp. Immunol. 51 (1) (2015) 10–21.
[24] T. Mekata, T. Kono, T. Yoshida, M. Sakai, T. Itami, Identification of cDNA encoding Toll receptor, MjToll gene from kuruma shrimp, *Marsupenaeus japonicas*, Fish Shellfsh Immunol 24 (1) (2008) 122–133.
[25] P.S. Hegde, I.R. White, C. Debouck, Interplay of transcriptomics and proteomics, Curr. Opin. Biotechnol. 14 (6) (2003) 647–651.
[26] W. Li, X. Tang, J. Xing, X. Sheng, W. Zhan, Proteomic analysis of differentially expressed proteins in *Fenneropenaeus chinensis* hemocytes upon white spot syndrome virus infection, PLoS One 9 (2) (2014) e89962.
[27] L. Zhu, X. Tang, J. Xing, X. Sheng, W. Zhan, Differential proteome of haemocyte subpopulations responded to white spot syndrome virus infection in Chinese shrimp *Fenneropenaeus chinensis*, Dev. Comp. Immunol. 84 (2018) 82–93.
[28] S.P. Antony, R. Philip, V. Joseph, I.B. Singh, Anti-lipopolysaccharide factor and crustin-III, the anti-white spot virus peptides in *Penaeus monodon*: control of viral infection by up-regulation, Aquaculture 319 (1–2) (2011) 11–17.
[29] B. Sun, Z. Wang, F. Zhu, The crustin-like peptide plays opposite role in shrimp immune response to *Vibrio alginolyticus* and white spot syndrome virus (WSSV) infection, Fish Shellfsh Immunol 66 (2017) 487–496.
[30] C.J. Coates, J. Nairn, Diverse immune functions of hemocyanins, Dev. Comp. Immunol. 45 (1) (2014) 43–55.

[31] M.A. Shu, C. Long, W.R. Dong, P. Zhang, B.P. Xu, X.L. Guo, The full-length cDNA cloning and expression profiles of 14-3-3 genes from the mud crab *Scylla paramamosain* Estampador, 1949, Crustaceana 88 (10–11) (2015) 1065–1078.
[32] X. Wei, X. Liu, J. Yang, J. Fang, H. Qiao, Y. Zhang, J. Yang, Two C-type lectins from shrimp *Litopenaeus vannamei* that might be involved in immune response against bacteria and virus, Fish Shellfsh Immunol 32 (1) (2012) 132–140.
[33] X.Y. Sun, Q.H. Liu, J. Huang, iTRAQ-based quantitative proteomic analysis of differentially expressed proteins in *Litopenaeus vannamei* in response to infection with WSSV strains varying in virulence, Lett. Appl. Microbiol. 67 (2) (2018) 113–122.
[34] H. Jiang, F. Li, J. Zhang, J. Zhang, B. Huang, Y. Yu, J. Xiang, Comparison of protein expression profiles of the hepatopancreas in *Fenneropenaeus chinensis* challenged with heat-inactivated *Vibrio anguillarum* and white spot syndrome virus, Mar. Biotechnol. 16 (1) (2014) 111–123.
[35] R.D. Rosa, M.A. Barracco, Antimicrobial peptides in crustaceans, Invertebr. Surviv. J. 7 (2) (2010) 262–284.
[36] H.P. Liu, R.Y. Chen, Q.X. Zhang, Q.Y. Wang, C.R. Li, H. Peng, K.J. Wang, Characterization of two isoforms of antiliopolysacchride factors (Sp-ALFs) from the mud crab *Scylla paramamosain*, Fish Shellfsh Immunol 33 (1) (2012) 1–10.
[37] P. Arosio, S. Levi, Ferritin, iron homeostasis, and oxidative damage, Free Radic. Biol. Med. 33 (4) (2002) 457–463.
[38] R. Rao, Y.B. Zhu, T. Alinejad, S. Tiruvayipati, K.L. Thong, J. Wang, S. Bhassu, RNA-seq analysis of *Macrobrachium rosenbergii* hepatopancreas in response to *Vibrio parahaemolyticus* infection, Gut Pathog. 7 (1) (2015) 6.
[39] F. Li, J. Xiang, Recent advances in researches on the innate immunity of shrimp in China, Dev. Comp. Immunol. 39 (1) (2013) 11–26.
[40] X.Q. Tang, X.L. Wang, W.B. Zhan, An integrin β subunit of Chinese shrimp *Fenneropenaeus chinensis* involved in WSSV infection, Aquaculture 368 (2012) 1–9.
[41] Y. Weinrauch, A. Zychlinsky, The induction of apoptosis by bacterial pathogens, Annu. Rev. Microbiol. 53 (1) (1999) 155–187.
[42] R. Rao, Y.B. Zhu, T. Alinejad, S. Tiruvayipati, K.L. Thong, J. Wang, S. Bhassu, RNA-seq analysis of *Macrobrachium rosenbergii* hepatopancreas in response to *Vibrio parahaemolyticus* infection, Gut Pathog. 7 (1) (2015) 6.
[43] B.B. Finlay, G. McFadden, Anti-immunology: evasion of the host immune system by bacterial and viral pathogens, Cell 124 (4) (2006) 767–782.
[44] S.A. Soto-Rodriguez, B. Gomez-Gil, R. Lozano-Olvera, M. Betancourt-Lozano, M.S. Morales-Covarrubias, Field and experimental evidence of *Vibrio parahaemolyticus* as the causative agent of acute hepatopancreatic necrosis disease of cultured shrimp (*Litopenaeus vannamei*) in Northwestern Mexico, Appl. Environ. Microbiol. 81 (5) (2015) 1689–1699.
[45] F. Zhu, X. Qian, X. Ma, Comparative transcriptomic analysis of crab hemocytes in response to white spot syndrome virus or *Vibrio alginolyticus* infection, Fish Shellfish Immunol. 80 (2018) 165–179.
[46] B. Verbruggen, L. Bickley, R. van Aerle, K. Bateman, G. Stentiford, E. Santos, C. Tyler, Molecular mechanisms of white spot syndrome virus infection and perspectives on treatments, Viruses 8 (1) (2016) 23.
[47] P.S. Gross, T.C. Bartlett, C.L. Browdy, R.W. Chapman, G.W. Warr, Immune gene discovery by expressed sequence tag analysis of hemocytes and hepatopancreas in the Pacific White Shrimp, *Litopenaeus vannamei*, and the Atlantic White Shrimp, *L. setiferus*, Dev. Comp. Immunol. 25 (7) (2001) 565–577.
[48] S. Li, F. Li, Z. Sun, X. Zhang, J. Xiang, Differentially proteomic analysis of the Chinese shrimp at WSSV latent and acute infection stages by iTRAQ approach, Fish Shellfsh Immunol 54 (2016) 629–638.
[49] X.Y. Sun, Q.H. Liu, J. Huang, iTRAQ-based quantitative proteomic analysis of differentially expressed proteins in *Litopenaeus vannamei* in response to infection with WSSV strains varying in virulence, Lett. Appl. Microbiol. 67 (2) (2018) 113–122.
[50] Z. Wang, F. Zhu, Minichromosome maintenance protein 7 regulates phagocytosis in kuruma shrimp *Marsupenaeus japonicas* against white spot syndrome virus, Fish Shellfsh Immunol 55 (2016) 293–303.
[51] F. Han, Z. Wang, X. Wang, Characterization of myosin light chain in shrimp hemocytic phagocytosis, Fish Shellfsh Immunol 29 (5) (2010) 875–883.
[52] D.P. Parrilla-Taylor, T. Zenteno-Savín, F.J. Magallon-Barajas, Antioxidant enzyme activity in pacific whiteleg shrimp (*Litopenaeus vannamei*) in response to infection with white spot syndrome virus, Aquaculture 380 (2013) 41–46.
[53] J. Jeswin, X.L. Xie, Q.L. Ji, K.J. Wang, H.P. Liu, Proteomic analysis by iTRAQ in red claw crayfish, *Cherax quadricarinatus*, hematopoietic tissue cells post white spot syndrome virus infection, Fish Shellfsh Immunol 50 (2016) 288–296.
[54] K. Hensley, K.A. Robinson, S.P. Gabbita, S. Salsman, R.A. Floyd, Reactive oxygen species, cell signaling, and cell injury, Free Radic. Biol. Med. 28 (10) (2000) 1456–1462.
[55] Q. Ren, R.R. Sun, X. Fan, J.X. Wang, A selenium-dependent glutathione peroxidase (Se-GPx) and two glutathione S-transferases (GSTs) from Chinese shrimp (*Fenneropenaeus chinensis*), Comp. Biochem. Physiol. C Toxicol. Pharmacol. 149 (2009) 613–623.